

Algorithm for Evaluating the Hourly Radiation Utilizability Function

D. R. Clark

S. A. Klein

W. A. Beckman

Solar Energy Laboratory,
University of Wisconsin,
Madison, Wis. 53706

A computationally simple algorithm is presented for evaluating the hourly utilizability function, ϕ , defined as the fraction of the long-term, monthly-average, hourly solar radiation incident on a surface which exceeds a specified threshold intensity. The algorithm was developed by correlating values of ϕ obtained by numerical integration of hourly radiation for three locations. The algorithm is shown to compare well both with a more complex analytical expression for ϕ developed recently and with results obtained numerically using many years of hourly horizontal radiation measurements in nine U.S. locations. In addition, the algorithm is shown to be applicable for surfaces of any orientation.

Introduction

Solar radiation utilizability, ϕ , is a solar radiation statistic, defined as the fraction of the total radiation incident on a surface which exceeds a specified intensity called the critical level. Utilizability was originally defined by Whillier [1] and later generalized by Liu and Jordan [2] as an approach to predicting the long-term average performance of flat-plate solar collectors. In this context, a critical radiation level is defined as the intensity at which thermal losses from the collector are equal to thermal gains and the net useful energy collection rate is zero; ϕ then represents the utilizable fraction of the total energy incident on the collector.

In recent years, the utilizability approach has been applied to a variety of solar energy applications [3, 4, 5, 6, 7]. For some applications the critical level is defined as an upper limit on useful radiation, rather than a lower limit. Thus, ϕ may represent either a useful energy fraction (utilizability) or a non-useful energy fraction (un-utilizability), depending on how the critical level is defined.

Since ϕ is a ratio of solar energy quantities, the time interval over which it is defined must be specified. Generally, ϕ is defined on a monthly-average basis over a period of an hour, e.g., the hour from 9 A.M. to 10 A.M. in January. A monthly-average daily value of ϕ , designated $\bar{\phi}$, can also be defined using a constant critical level throughout the day. Simple algorithms exist [8, 9, 10] for evaluating the constant critical level daily utilizability function.

Until recently, evaluation of the hourly utilizability function, ϕ , required the use of the generalized ϕ -curves of Liu and Jordan [2]. Since analytical expressions are not available for these graphs, the use of the hourly approach has been limited. Hourly utilizability has two distinct advantages over daily utilizability. First, it allows the critical level to be defined independently for each hour of the day, an important consideration for some applications. A monthly-average daily utilizability with a nonuniform critical level, $\bar{\phi}$, can then be

evaluated. Second, it greatly facilitates calculation of utilizability for surfaces that do not face south, since geometric factors can be assumed constant for each hour and need not be integrated over time. A simple algorithm for evaluating the hourly utilizability function is presented in this paper.

A defining equation for ϕ can be written in terms of the probability distribution of insolation levels

$$\phi = \frac{\int_{I_c}^{I_{T,\max}} (I_T - I_c) P(I_T) dI_T}{\int_{I_{T,\min}}^{I_{T,\max}} I_T P(I_T) dI_T} \quad (1)$$

where I_T is the hourly radiation incident on the tilted surface; $I_{T,\max}$ is the maximum observed value of I_T ; $I_{T,\min}$ is the minimum observed value of I_T ; I_c is the critical radiation level; and $P(I_T)$ is the radiation frequency distribution which gives the probability of insolation at level I_T occurring.

Liu and Jordan [2] have shown that the shape of radiation frequency distribution curves can be treated as a unique function of \bar{K} , the monthly-average clearness index¹, independent of location and season.

Huget [10] has rewritten equation (1) in terms of hourly clearness indices and has performed the integration analytically using a curve fit to the generalized clearness index frequency distributions of Liu and Jordan and assuming that the maximum observed clearness index can be treated as a constant for all hours and locations. The resulting equation for ϕ is algebraically complex, but is suitable for computer implementation and applicable for any collector orientation.

A simpler equation for ϕ can be obtained by directly correlating values of ϕ calculated from long-term weather data, rather than by integrating the frequency distribution correlation. In this paper, a new correlation for ϕ is

Contributed by the Solar Energy Division for publication in the JOURNAL OF SOLAR ENERGY ENGINEERING. Manuscript received by the Solar Energy Division September 23, 1982.

¹ \bar{K} is the ratio of monthly-average daily total radiation to extraterrestrial radiation, both on a horizontal surface.

presented, based on the results of hourly calculations using many years of actual horizontal radiation data for a few surface orientations in each of three locations. Results of the correlation are compared with utilizability values calculated from actual radiation data for these three and six other locations and from other correlations [10, 11].

Although the correlation is based on data for surfaces facing directly towards the equator, it is shown to be applicable with comparable accuracy to surfaces with other azimuthal orientations. The utilizability function can also be used to estimate the fractional time in which the solar radiation is greater than the critical level, as described in Appendix A.

Data Base for Correlation

The data on which the correlation is based are derived from 23 years of hourly horizontal radiation measurements in Madison, Wisconsin, 23 years in Albuquerque, New Mexico, and 15 years in Seattle, Washington [12]. These locations were selected to cover a broad range of average hourly clearness index values and a reasonable range of latitudes. The resulting correlation for ϕ is then compared to results obtained from many years of hourly data for Columbia, Missouri; Fort Worth, Texas; Miami, Florida; New York, New York; Phoenix, Arizona; and Washington, D.C.

Values of ϕ were obtained by numerical integration of long-term weather data. Tilted-surface radiation was calculated from the horizontal data using the isotropic sky model of Liu and Jordan [13]

$$I_T/I = R = (1 - I_d/I)R_b + I_d/I \left(\frac{1 + \cos\beta}{2} \right) + \rho \left(\frac{1 - \cos\beta}{2} \right) \quad (2)$$

with the diffuse fraction correlation recommended by Erbs [14]

$$I_d/I = \begin{cases} 1.0 - 0.09k, & k \leq 0.22 \\ 0.9511 - 0.1604k + 4.388k^2 - 16.638k^3 \\ \quad + 12.336k^4, & 0.22 < k < 0.80 \\ 0.165, & k > 0.80 \end{cases} \quad (3)$$

where k is the hourly clearness index²

$$k = I/I_0 \quad (4)$$

ϕ was calculated as a function of X_c , a dimensionless critical ratio defined as the ratio of the critical intensity to the monthly-average radiation value on the surface of interest.

$$X_c = I_c/\bar{I}_T \quad (5)$$

For each sunlit hour of each month, ϕ was calculated at 50 values of X_c in equal increments from $X_c = 0$ to $X_c = 2.45$. Long-term averages of \bar{I}_T and \bar{k} were obtained at the same time for use in developing the correlation.

Attention was restricted to hours for which R_b is positive throughout the hour for the whole month. Hours for which this was not true represent low radiation values, making accurate knowledge of ϕ unimportant. The correlation is based entirely on data for south-facing surface slopes of 0, 60 and 90 deg in Madison, 0 and 90 deg in Albuquerque, and 30 deg in Seattle.

To provide data for comparisons with the utilizability correlation (which were not used in its development) values of ϕ were obtained numerically for south-facing surfaces in six other locations at several angles of tilt. Values of ϕ were also obtained for a number of nonzero azimuth orientations in all nine locations. These comparisons demonstrate the generality of the utilizability correlation presented here with regard to location and orientation.

² k is the clearness index for a particular hour, while \bar{k} is the monthly-average hourly clearness index which is the average of all observations in a month for the hour, e.g., 9-10 A.M.

Nomenclature

- | | |
|--|--|
| <p>a = coefficient appearing in the correlation for ϕ in equation (6); coefficient appearing in equation (B2)</p> <p>b = coefficient appearing in equation (B2)</p> <p>I = instantaneous (or hourly average) solar radiation on a horizontal surface, W/m^2</p> <p>\bar{I} = monthly-average value of I, W/m^2</p> <p>I_c = critical radiation level, W/m^2</p> <p>I_d = instantaneous (or hourly average) diffuse solar radiation on a horizontal surface, W/m^2</p> <p>\bar{I}_d = monthly-average value of I_d, W/m^2</p> <p>I_0 = instantaneous (or hourly average) extraterrestrial radiation on a horizontal surface, W/m^2</p> <p>\bar{I}_0 = monthly-average value of I_0, W/m^2</p> <p>I_T = instantaneous (or hourly average) solar radiation on a tilted surface, W/m^2</p> <p>$I_{T, \max}$ = maximum value of I_T, W/m^2</p> <p>$I_{T, \min}$ = minimum value of I_T, W/m^2</p> <p>\bar{I}_T = monthly-average value of I_T, W/m^2</p> <p>\bar{H} = monthly-average daily solar radiation on a horizontal surface, J/m^2-day</p> <p>\bar{H}_d = monthly-average daily diffuse solar radiation on a horizontal surface, J/m^2-day</p> <p>\bar{H}_0 = monthly-average daily extraterrestrial radiation on a horizontal surface, J/m^2-day</p> <p>k = clearness index defined in equation 4</p> <p>\bar{k} = monthly-average value of k</p> <p>\bar{K} = monthly-average daily clearness index</p> | <p>\dot{P} = power consumption of pumps, etc., W</p> <p>\bar{P}_i = monthly-averaged energy consumed by pumps etc. during time interval; J</p> <p>$P(I_T)$ = probability distribution of I_T values</p> <p>\bar{R} = ratio of monthly-average instantaneous radiation on a tilted surface to that on a horizontal surface given by equation (B7)</p> <p>R_b = ratio of beam radiation on a tilted surface to that on a horizontal surface</p> <p>\bar{t}_i = monthly-average fraction of time interval i in which the solar radiation exceeds the critical level</p> <p>X_c = dimensionless critical level given by equation (5)</p> <p>X_m = dimensionless variable defined by equation (10)</p> <p>β = slope of surface, deg</p> <p>γ = surface azimuth angle, deg (positive values for west-facing surface, 0 for south-facing)</p> <p>ϕ = solar declination, deg</p> <p>Δt = length of time interval, s</p> <p>δ = solar radiation utilizability for a particular time based on instantaneous (or hourly-average) data</p> <p>$\bar{\phi}$ = monthly-average daily utilizability defined by equation (11)</p> <p>$\bar{\phi}$ = monthly-average daily utilizability</p> <p>ρ = ground reflectance</p> |
|--|--|

Table 1 Unavoidable error from the use of equation (6)
 Madison, Slope = 60°, Azimuth = 0°, Morning Hours
 X_m Selected for Each Hour by Nonlinear Regression

Month	Minimum rms Error in ϕ (%)			
	Hour			
	8-9	9-10	10-11	11-12
Jan	1.72	1.82	1.61	1.68
Feb	2.40	2.25	1.84	1.54
Mar	1.60	1.64	1.64	1.62
Apr	1.28	1.37	1.62	1.50
May	0.95	1.09	1.09	0.89
Jun	0.75	0.92	0.85	0.61
Jul	0.81	0.73	0.57	0.57
Aug	0.93	0.79	0.59	0.71
Sep	1.38	1.58	1.47	1.27
Oct	0.91	1.49	1.80	1.86
Nov	0.64	1.46	1.68	1.87
Dec	0.41	1.51	1.63	1.58

Empirical Correlation Procedure

Curves of ϕ versus X_c derived from long-term hourly weather data as described above were fitted to an equation of the following form

$$\phi = \begin{cases} 0, & X_c \geq X_m \\ (1 - X_c/X_m)^2, & X_m = 2 \\ | |a| - [a^2 + (1 + 2a)(1 - X_c/X_m)^2]^{1/2} | & \text{otherwise} \end{cases} \quad (6)$$

where

$$a = (X_m - 1)/(2 - X_m) \quad (7)$$

and X_m is the only degree of freedom in this equation. A single value of X_m defines a curve of ϕ versus X_c .

Mathematically, equation (6) describes a segment of a conic section (hyperbola or ellipse) with a slope of -1 and a value of 1 at $X_c = 0$, and a slope and value of 0 at $X_c = X_m$. This form was chosen in an effort to describe the utilizability function over the entire range of possible critical levels. The slope of the utilizability versus X_c curve becomes -1 as X_c (and thus I_c) approach zero since I_T , the solar radiation for any particular hour, is then always greater than I_c . At the other extreme, ϕ approaches a limiting value of 0 with a slope of zero as the critical level approaches $I_{T, \max}$. This behavior also implies that

$$X_m = I_{T, \max} / \bar{I}_t \quad (8)$$

Attempts to calculate ϕ from equations (6-8), using $I_{T, \max}$ estimated from basic principles and various simplifying assumptions, yielded poorer agreement than the purely empirical correlation for X_m described below.

For each location and slope, for each hour of each month, a nonlinear regression program was used to find the value of X_m which minimized the root-mean-square (rms) error of ϕ , i.e., the standard deviation of the differences between the values of ϕ obtained from many years of weather data and those from equation (6). These optimum values of X_m are designated $X_{m, \text{opt}}$.

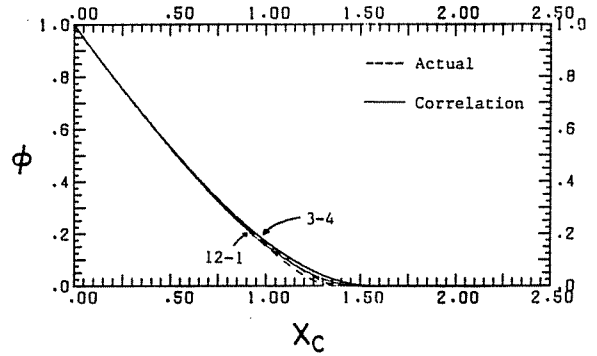


Fig. 1 Comparison of equation (6) (solid lines) with long-term hourly calculations for a 60 deg south-facing surface in Madison, Wis. during June for 12AM-1PM and 3-4PM

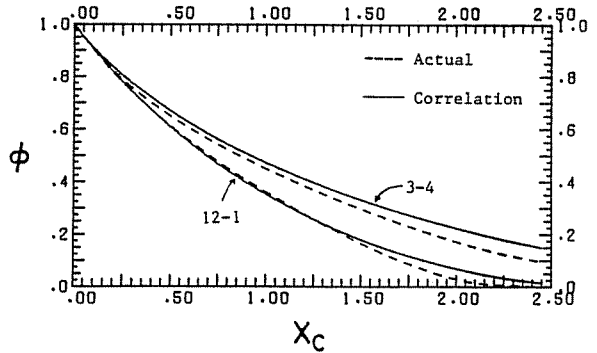


Fig. 2 Comparison of equation (6) (solid lines) with long-term hourly calculations for a 60 deg south-facing surface in Madison, Wis. during December for 12AM-1PM and 3-4PM

When $X_{m, \text{opt}}$ is used in equation (6) to estimate ϕ , the residual error is a minimum. The difference in the value of ϕ calculated from actual data and that obtained from equation (6) using $X_{m, \text{opt}}$ represents an unavoidable error in the form of the correlation. Table 1 lists values of the minimum rms error for morning hours from 8 A.M. to noon for a surface tilted south at 60 deg in Madison. Each number in the table represents the standard deviation of 25 to 50 observations, scaled such that ϕ varies from 0 to 100. The errors are small and essentially independent of time of day, but they tend to be larger for winter months than for summer months. Similar results are obtained for afternoon hours and for other tilts and locations. These results demonstrate that the form of equation (6) is adequate provided that a correlation for X_m can be found.

A large number of different correlations for X_m in terms of solar and geometric parameters were investigated. The best model found for X_m is of the form

$$X_m = C_1 + C_2 \bar{R} / \bar{k}^2 - C_3 (\cos \beta) / \bar{k}^2 - C_4 \bar{k} / (\cos \delta)^2 \quad (9)$$

where

$$\bar{R} = \bar{I}_T / \bar{I}$$

β = slope of surface

δ = declination

The constants were evaluated for the six sets of data for south-facing surfaces for all 12 months. Again, all hours between 6 A.M. and 6 P.M. for which R_b is positive throughout the hour were considered. Values of X_c were taken in increments of 0.2. A total of 6329 observations were included in the regression. The final correlation is given by equation (6) with X_m given by

Table 2 Comparison of correlation results and long-term weather results

Azimuth	Location	Slope	No. of Observations	Present Correlation (Eq. (6))		Huguet Correlation	
				Actual E, I_T	Estimated E, I_T	Actual E, I_T	Estimated E, I_T
				Mean Bias Error of ϕ (%)	rms Error of ϕ (%)	Mean Bias Error of ϕ (%)	rms Error of ϕ (%)
0°	Albuquerque	0°	3847	-0.35	1.58	-0.42	1.82
0°	Albuquerque	90°	3390	-0.74	2.14	-0.81	4.26
0°	Madison	0°	4797	-0.46	2.01	-0.47	1.74
0°	Madison	60°	4579	-0.23	2.20	-0.45	3.57
0°	Madison	90°	4423	0.26	2.33	-0.12	4.14
0°	Seattle	30°	5158	1.16	3.74	1.16	3.54
0°	Seattle	90°	4610	2.70	4.93	2.81	5.62
45°	Madison	43°	4078	-0.76	3.38	-1.93	4.52
90°	Madison	90°	2477	-0.99	3.21	-2.32	6.52

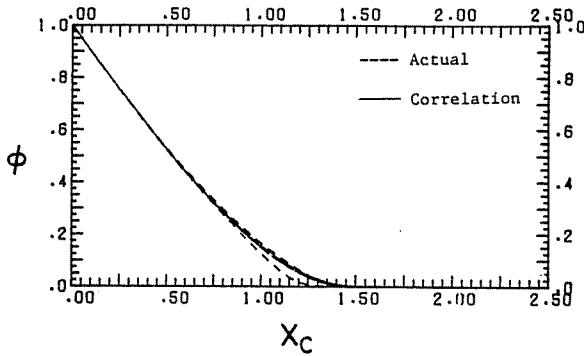


Fig. 3 Comparison of equation (6) (solid lines) with long-term hourly calculations for a 60 deg south-facing surface in Seattle, Wash. during June for 12AM-1PM and 3-4PM

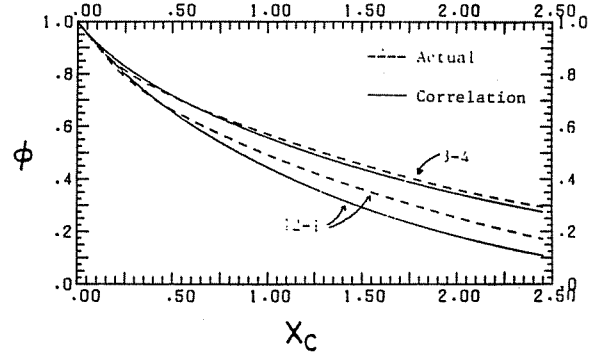


Fig. 4 Comparison of equation (6) (solid lines) with long-term hourly calculations for a 60 deg south-facing surface in Seattle, Wash. during December for 12AM-1PM and 3-4PM

$$X_m = 1.85 + 0.169\bar{R}/\bar{k}^2 - 0.0696(\cos\beta)/\bar{k}^2 - 0.981\bar{k}/(\cos\delta)^2 \quad (10)$$

Correlation Results and Comparisons

The values of \bar{k} and \bar{I}_T used in developing equation (10) are long-term averages calculated from the hourly weather data used to calculate ϕ . In practice, however, the correlation will be used with \bar{k} and \bar{I}_T estimated from the monthly-average daily clearness index, \bar{K} . It is important to determine how the accuracy of the present correlation is affected by the use of these estimates. It is also instructive to compare the present correlation with the more complicated expression for ϕ presented by Huguet.

Using published [15] values of \bar{K} , the parameters \bar{k} and \bar{I}_T were calculated as outlined in Appendix B, and were used with equation (6) to calculate ϕ . Figures 1-4 compare the ϕ -curves obtained from long-term weather data and the correlation given by equation (6) for a few sets of conditions. The comparisons with Huguet's correlation appear identical. The two methods are of very similar accuracy; both agree closely with results from long-term weather data.

Table 2 lists the mean bias error and the standard deviation of the error (i.e., rms error) in estimating ϕ with equation (6). A positive mean bias error indicates that on the average, over all months, hours, and critical levels considered, ϕ is underpredicted. Results are presented for the \bar{k} and \bar{I}_T and for both the present correlation and Huguet's method using appropriate estimated values. The use of estimated rather than actual radiation parameters increases the uncertainty for steeply tilted surfaces by as much as 3 percent. For horizontal or slightly tilted surfaces, the effect on the uncertainty is small and may either increase or decrease the rms error.

The first six rows of Table 2 represent the data used in

evaluating the constants of the present correlation. For these data, equation (6) is consistently (but slightly) more accurate than the method of Huguet. The comparison is not entirely fair, however, since equation (6) was specifically fitted to these data, while Huguet's correlation was derived from a different set of data. The present correlation is more accurate for two of the three remaining lines in the table. Perhaps more significant is the correspondence between the uncertainties of the two methods. To a good approximation, the rms error of one method could be used to predict the rms error of the other method. The consistency of this relationship for the three locations considered suggests that the same may hold for other locations as well.

The rms errors reported in Table 2 are somewhat misleading, since the largest errors in the calculated values of ϕ are generally observed for hours near sunrise and sunset when the amount of energy involved is small. This is shown in Table 3, which gives rms errors of the present correlation for each morning hour of each month for a vertical south-facing surface in Albuquerque. Similar patterns are obtained for afternoon hours and for other slopes and locations.

An energy-weighted comparison is provided in Table 4. The uncertainties in estimating \bar{I}_T alone are included in the table. The values are somewhat inflated by occasional small (± 0.02) discrepancies between the published value of \bar{K} used in this comparison and values obtained from the hourly data used to calculate ϕ .

A significant feature of the data in Table 4 is the strong relationship between the uncertainty of $\bar{I}_T\phi$ from either method and the uncertainty of \bar{I}_T alone. For all locations and slopes examined, the present correlation is slightly more accurate than Huguet's method in estimating $\bar{I}_T\phi$, which represents energy above the critical level. These differences, however, are quite small, and may be reversed for other

locations. The primary advantage of the present correlation over Huget's is its simplicity.

Monthly-average daily utilizability can be found as a radiation-weighted average of hourly utilizability from equation (6)

$$\bar{\phi} = \frac{\sum \bar{I}_T \phi}{\sum \bar{I}_T} \quad (11)$$

The symbol $\bar{\phi}$ rather than ϕ is used here to indicate that the critical level is not necessarily constant over the day, but may

vary from hour to hour. A comparison between $\bar{\phi}$ from equation (11), ϕ from hourly Typical Meteorological Year (TMY) data [16], and $\bar{\phi}$ from [11], is provided in Table 5. A different constant critical level was used for each month to obtain a broad range of values of ϕ . The rms error of equation (11) relative to the TMY data is 1.8 percent. The method of Theilacker and Klein [11] is of similar accuracy, but is limited to south-facing surfaces and constant daily critical levels.

The results for Boston in Table 5 suggest that equations (6) and (11) are not restricted to south-facing surfaces but can be used to evaluate utilizability for surfaces of any orientation. Additional support for this hypothesis is provided in Table 6 in which rms and mean bias errors of $\bar{\phi}$ from equation (11) relative to values of ϕ calculated using 15 to 23 years of hourly weather data are presented for a variety of nonsouth surface orientations for nine locations. Ten critical levels, chosen to vary X_c from 0 to 2.5 were used in these calculations.

The computational effort needed to evaluate $\bar{\phi}$ using equation (11) can be significant since values of ϕ for each hour between sunrise and sunset are involved in the summation. The use of hourly time intervals in equation (11) is, however, arbitrary. The computational effort can be reduced if a smaller number of longer time intervals are used in equation (11). Shown in Table 7 are rms and mean bias errors in $\bar{\phi}$ (relative to values obtained by numerical integration of long-term data) calculated using equation (11) with the period between sunrise and sunset divided into 12, 6, 5, 4, and 3 equal intervals. The results were computed at constant daily critical levels of 20, 100, 200, 320, and 460 W/m², for slopes of 0, 30, 60, and 90 deg, and for azimuth angles of 0, 45, and 90 deg. Thus, 600 values of $\bar{\phi}$ were obtained by each method for each of the six locations.

Table 3 RMS errors (%) of present correlation for a vertical south-facing surface in Albuquerque

Month	TIME (AM)				
	7 - 8	8 - 9	9 - 10	10 - 11	11-12
Jan	—	3.9	3.0	2.6	2.1
Feb	6.1	4.9	4.0	3.1	2.5
Mar	4.6	3.6	2.8	2.0	1.1
Apr	3.4	3.0	2.8	2.1	1.3
May	—	4.5	3.6	2.9	2.2
Jun	—	—	1.9	1.6	1.3
Jul	—	3.8	1.5	0.6	0.3
Aug	1.2	3.0	1.6	1.3	1.2
Sep	5.0	2.6	1.8	1.6	1.9
Oct	17.0	6.7	3.6	2.7	2.4
Nov	—	11.7	4.9	2.6	2.0
Dec	—	8.5	3.4	2.4	1.9

Table 4 Energy-weighted comparisons of correlations for ϕ

Azimuth	Location	Slope	No. of Observations	$(\bar{T}_{T,act} - \bar{T}_{T,est})$				$(\bar{T}_{T,act} - \bar{T}_{T,est})$		
				Present Correlation		Huget Correlation		No. of Observations	Mean Bias Error	rms Error
				Mean Bias Error	rms Error	Mean Bias Error	rms Error			
0°	Albuquerque	0°	3847	1 W/m ²	16 W/m ²	8 W/m ²	21 W/m ²	124	4 W/m ²	23 W/m ²
0°	Albuquerque	90°	3390	0	25	10	29	106	7	30
0°	Madison	0°	4797	0	7	4	11	122	1	8
0°	Madison	60°	4579	1	18	8	23	112	4	22
0°	Madison	90°	4423	2	18	5	21	106	2	22
0°	Seattle	30°	5158	6	20	11	26	120	3	29
0°	Seattle	90°	4610	9	20	11	23	106	3	23
45°	Madison	43°	4078	-5	18	7	20	103	1	16
90°	Madison	90°	2477	-11	33	-7	34	61	-10	39

Table 5 Comparison of daily utilizability from equation (11) and from (TMY) data

Month	I_c (W/m ²)	$\bar{\phi}$	Phoenix, AZ.			Boston, MA*			Medford, OR			
			Eq. (11)	Ref. [11]	TMY	Eq. (11)	TMY	Eq. (11)	Ref. [11]	TMY		
Jan	40	.61	.92	.92	.92	.37	.84	.83	.33	.83	.83	.79
Feb	200	.67	.69	.68	.67	.41	.49	.52	.44	.48	.48	.47
Mar	360	.70	.51	.48	.50	.45	.32	.35	.50	.24	.20	.28
Apr	80	.74	.87	.88	.87	.43	.78	.78	.54	.73	.73	.72
May	240	.78	.66	.66	.65	.47	.49	.52	.59	.30	.27	.29
Jun	400	.75	.43	.42	.42	.52	.30	.32	.64	.04	.06	.03
Jul	120	.68	.79	.79	.79	.49	.71	.71	.71	.59	.61	.57
Aug	280	.69	.58	.56	.57	.47	.44	.43	.66	.34	.29	.32
Sep	440	.72	.42	.40	.41	.50	.27	.28	.63	.19	.16	.18
Oct	160	.69	.76	.75	.75	.45	.60	.60	.52	.61	.60	.59
Nov	320	.68	.52	.50	.50	.38	.26	.26	.39	.29	.25	.31
Dec	480	.59	.28	.24	.24	.35	.08	.06	.27	.05	.03	.07
Year			.62	.61	.62		.47	.48		.39	.38	.38
Latitude			33.43°				42.37°			42.38°		
Slope			33.43°				42.37°			90°		
Azimuth			0°				-45°			0°		

*The method of Ref. [11] is not applicable for non-zero azimuth angle.

Table 6 Accuracy of $\bar{\phi}$ from equation (11) relative to $\bar{\phi}$ from long-term hourly data

Location	RMS Errors					
	$\beta=90, \gamma=0$	$\beta=\text{lat}, \gamma=0$	$\beta=90, \gamma=45$	$\beta=90, \gamma=90$	$\beta=90, \gamma=180$	$\beta=\text{lat}, \gamma=45$
Madison, WI	0.026	0.023	0.029	0.044	0.047	0.023
Washington, D.C.	0.023	0.022	0.033	0.050	0.041	0.025
Albuquerque, NM	0.019	0.017	0.027	0.042	0.026	0.017
Miami, FL	0.047	0.051	0.061	0.068	0.026	0.052
Fort Worth, TX	0.026	0.022	0.029	0.038	0.040	0.023
Columbia, MO	0.033	0.025	0.028	0.027	0.047	0.023
New York, NY	0.025	0.025	0.038	0.057	0.041	0.028
Phoenix, AZ	0.031	0.026	0.043	0.055	0.019	0.028
Seattle, WA	0.054	0.037	0.041	0.024	0.053	0.031

Location	Mean Bias Errors					
	$\beta=90, \gamma=0$	$\beta=\text{lat}, \gamma=0$	$\beta=90, \gamma=45$	$\beta=90, \gamma=90$	$\beta=90, \gamma=180$	$\beta=\text{lat}, \gamma=45$
Madison, WI	-0.002	0.001	0.017	0.037	0.041	0.011
Washington, DC	0.005	0.008	0.023	0.043	0.031	0.015
Albuquerque, NM	0.002	0.005	0.020	0.035	0.013	0.011
Miami, FL	0.029	0.044	0.052	0.059	-0.005	0.045
Fort Worth, TX	-0.007	-0.004	0.010	0.028	0.034	0.001
Columbia, MO	-0.017	-0.013	-0.005	0.015	0.042	-0.008
New York, NY	0.005	0.007	0.026	0.049	-0.030	0.016
Phoenix, AZ	0.013	0.016	0.030	0.043	0.009	0.019
Seattle, WA	-0.039	-0.026	-0.026	0.006	0.047	-0.019

Table 7 Effect of the number of time intervals on the accuracy of $\bar{\phi}$ from equation (11)

Location	RMS Errors				
	N = 12	N = 6	N = 5	N = 4	N = 3
Columbia, MO	.021	.024	.026	.030	.042
Ft. Worth, TX	.021	.021	.023	.026	.037
Miami, FL	.043	.039	.037	.035	.032
New York, NY	.023	.023	.024	.026	.035
Phoenix, AZ	.027	.024	.025	.024	.033
Washington, DC	.021	.020	.020	.022	.031
Combined Data	.027	.026	.026	.027	.035

Location	Mean Bias Errors				
	N = 12	N = 6	N = 5	N = 4	N = 3
Columbia, MO	.007	.012	.014	.018	.029
Ft. Worth, TX	-.001	.004	.006	.010	.022
Miami, FL	-.032	-.028	-.025	-.021	-.009
New York, NY	-.003	.001	.004	.007	.018
Phoenix, AZ	-.016	-.011	-.010	-.006	.006
Washington, DC	-.008	-.004	-.001	-.003	.014
Combined Data	-.009	-.004	-.002	-.002	.013

Table 8 Hourly results from sample calculation

Hour	\bar{k}	$\bar{I}_T (\text{W/m}^2)$	$\bar{I}_T (\text{W/m}^2)$	ϕ	$\bar{I}_\phi (\text{W/m}^2)$
8-9 AM	.335	84.3	189.7	.829	157.3
9-10 AM	.378	162.1	282.0	.871	245.5
10-11 AM	.408	226.1	342.5	.890	304.6
11-12 AM	.423	262.2	351.1	.893	318.8
12-1 PM	.423	262.2	323.5	.881	285.1
1-2 PM	.408	226.1	250.9	.849	212.9
2-3 PM	.378	162.1	157.2	.766	120.4
3-4 PM	.335	84.3	63.3	.480	30.4
SUM			1966.		1675.

$$X_m = 4.39$$

From equation (6)

$$a = -1.418$$

$$\phi = 0.829$$

The calculations are then repeated for each hour of the day. \bar{I} and \bar{k} need only be calculated for morning hours, since horizontal radiation is assumed to be symmetric about noon. \bar{I}_T must be calculated for all hours if the surface azimuth angle is nonzero, as in this example. ϕ must also be calculated for all hours if the azimuth angle is nonzero or if the hourly critical levels are not symmetric about noon. Results of these calculations are given in Table 8. The monthly-average daily utilizability, $\bar{\phi}$, is then given by

$$\bar{\phi} = (\Sigma \bar{I}_T \phi) / (\Sigma \bar{I}_T) = 1675 / 1966 = 0.85$$

Acknowledgment

The authors thank D. G. Erbs for his assistance in the calculation of utilizability values based on long-term hourly weather data. This work has been supported by the Solar Heating and Cooling Research and Development Branch, Office of Conservation and Solar Applications, U.S. Department of Energy.

References

- 1 Whillier, A., "Solar Energy Collection and Its Utilization for House Heating," PhD thesis, Mechanical Engineering, Massachusetts Institute of Technology, Cambridge, Mass., 1953.
- 2 Liu, B. Y. H., and Jordan, R. C., "A Rational Procedure for Predicting the Long-Term Average Performance of Flat Plate Solar Energy Collectors," *Solar Energy*, Vol. 7, 1963, p. 53.
- 3 Klein, S. A., and Beckman, W. A., "A General Design Method for Closed-Loop Solar Energy Systems," *Solar Energy*, Vol. 22, 1979, p. 269.

The results for Miami are of particular interest. The large negative mean bias error when 12 intervals are used can be attributed to the unusual uniformity of Miami weather. Reducing the number of intervals to 3 in this case largely compensates for the mean bias error, decreasing the rms error from .043 to .032. A similar but smaller effect is seen when the number of intervals is reduced from 12 to 6 for other locations which have a negative mean bias error at $N = 12$. In general, dividing the hours of daylight into 12 intervals appears unnecessary; overall, the use of 4 to 6 intervals results in essentially no change in accuracy. When the critical level varies through the day, this variability should be considered in deciding on a number of intervals to use.

Example

Calculate the value of $\bar{\phi}$ in January for a surface in Boston, Mass. ($\bar{K} = 0.396$) at an azimuth angle of -45 deg (south-east), a slope equal to the latitude (42.37 deg), and a critical level of 40 W/m^2 .

For January in Boston the first hour after sunrise is the hour from 8 A.M. to 9 A.M. The declination, δ , is -20.9 deg in January, and the sunset hour angle, ω_s , is 69.6 deg. Using the procedure outlined in Appendix B with a ground reflectance equal to 0.2, the following hourly radiation parameters are found for this hour

$$\bar{k} = 0.335 \quad \bar{R} = 2.25$$

$$\bar{I} = 84.3 \text{ W/m}^2 \quad \bar{I}_T = 189.7 \text{ W/m}^2$$

From equation (5)

$$X_c = I_c / \bar{I}_T = (40 \text{ W/m}^2) / (189.7 \text{ W/m}^2) = 0.211$$

From equation (10)

4 Monsen, W. A., Klein, S. A., and Beckman, W. A., "Prediction of Direct Gain Solar Heating System Performance," *Solar Energy*, Vol. 27, 1981, p. 143.

5 Braun, J. E., Klein, S. A., and Mitchell, J. W., "Seasonal Storage of Energy in Solar Heating," *Solar Energy*, Vol. 26, 1981, p. 403.

6 Siegel, M. D., Klein, S. A., and Beckman, W. A., "A Simplified Method for Estimating the Monthly-Average Performance of Photovoltaic Systems," *Solar Energy*, Vol. 26, 1981, p. 413.

7 Clark, D. R., Klein, S. A., and Beckman, W. A., "A Method for Estimating the Performance of Photovoltaic Systems," submitted to *Solar Energy Journal*.

8 Klein, S. A., "Calculation of Flat-Plate Collector Utilizability," *Solar Energy*, Vol. 21, 1978, p. 393.

9 Collares-Pereira, M., and Rabl, A., "Simple Procedure for Predicting Long-Term Average Performance of Nonconcentrating and of Concentrating Solar Collectors," *Solar Energy*, Vol. 23, 1979, p. 235.

10 Huet, R. G., "A Method for Estimating the Daily Utilizability of Flat-Plate Solar Collectors," M.S. thesis, Mechanical Engineering, University of Waterloo, Ontario, 1981.

11 Mitchell, J. C., Theilacker, J. C., and Klein, S. A., "Calculation of Monthly Average Collector Operating Time and Parasitic Energy Requirements," *Solar Energy*, Vol. 26, 1981, pp. 555-558.

12 Solmet, "Hourly Solar Radiation Surface Meteorological Observations," TD-9724, 1979.

13 Liu, B. Y. H., and Jordan, R. C., "The Interrelationship and Characteristic Distribution of Direct, Diffuse and Total Solar Radiation," *Solar Energy*, Vol. 4, 1960, p. 1.

14 Erbs, D. G., "Estimation of the Diffuse Radiation Fraction for Hourly, Daily and Monthly Average Global Radiation," *Solar Energy*, Vol. 28, 1982, p. 293.

15 Duffie, J. A., and Beckman, W. A., *Solar Engineering of Thermal Process*, Wiley-Interscience, New York, 1980.

16 Solmet, Typical Meteorological Year, Tape Deck 9734, NOAA, Environmental Data Service, NCC, Ashville, N.C.

17 Collares-Pereira, M., and Rabl, A., "The Average Distribution of Solar Radiation-Correlations Between Daily and Hourly Insolation Values," *Solar Energy*, Vol. 22, 1979, p. 155.

APPENDIX A

Fractional Operating Time and Parasitic Power

Mitchell et al. [11] have shown that the average daily time during which incident radiation exceeds the critical level can be calculated from the daily utilizability function. For collectors with on/off control, this represents the average daily operating time and can be used to calculate pumping power. Their analysis can be applied directly to the hourly utilizability function, yielding

$$\bar{t}_i = -\frac{d\phi_i}{dX_c}$$

$$= \begin{cases} 0 & \text{for } X_c \geq X_m \\ 1 - X_c/X_m & \text{for } X_m = 2 \\ \left| \frac{X_m - X_c}{X_m(2 - X_m)} \right| [a^2 + (1 + 2a)(1 - X_c/X_m)^2]^{-1/2} & \text{otherwise} \end{cases}$$

where \bar{t}_i is the average fraction of time interval i (for which X_m is defined) during which the incident radiation exceeds the

critical level. For collectors with on/off control, the pumping energy requirement, \bar{P}_i , for the time interval, Δt , is the product of the fractional operating time, the power consumption when the pump is on, \dot{P} , and the length of the time interval.

$$\bar{P}_i = \bar{t}_i \dot{P} \Delta t \quad (\text{A1})$$

Again, monthly-average daily results can be obtained by summing or averaging results for each time interval over the day.

APPENDIX B

Estimation of Hourly Radiation Parameters

The monthly-average hourly clearness index, \bar{k} , is defined as the ratio of monthly-average hourly horizontal to extraterrestrial radiation

$$\bar{k} = \bar{I} / \bar{I}_0 \quad (\text{B1})$$

\bar{k} can be estimated from the monthly-average daily clearness index, \bar{K} , using a correlation developed by Collares-Pereira and Rabl [17]

$$\bar{k} = \bar{K} (a + b \cos \omega) \quad (\text{B2})$$

where

$$a = 0.409 + 0.5016 \sin(\omega_s - 60 \text{ deg})$$

$$b = 0.6609 - 0.4767 \sin(\omega_s - 60 \text{ deg})$$

and ω_s is the sunset hour angle. Monthly-average hourly extraterrestrial radiation, \bar{I}_0 , can be calculated from equation (1.8.4) of [15]; monthly-average hourly horizontal radiation, \bar{I} , is then given by

$$\bar{I} = \bar{I}_0 \bar{k} \quad (\text{B3})$$

Liu and Jordan [13] relate average hourly to daily diffuse radiation by

$$\bar{I}_d / \bar{H}_d = \bar{I}_0 / \bar{H}_0 \quad (\text{B4})$$

Combining equations (B4) and (B2),

$$\bar{I}_d / \bar{I} = (\bar{H}_d / \bar{H}) (a + b \cos \omega)^{-1} \quad (\text{B5})$$

In the present study, the daily average diffuse fraction correlation of Erbs [14] has been used

$$\bar{H}_d / \bar{H} = 1.317 - 3.023 \bar{K} + 3.372 \bar{K}^2 - 1.76 \bar{K}^3 \quad (\text{B6})$$

The ratio of average hourly tilted-surface to average horizontal radiation, \bar{R} , is given by

$$\bar{R} = (1 - \bar{I}_d / \bar{I}) R_b + (\bar{I}_d / \bar{I}) \left(\frac{1 + \cos \beta}{2} \right) + \rho \left(\frac{1 - \cos \beta}{2} \right) \quad (\text{B7})$$

where β is the slope of the surface, ρ is the ground reflectance, and R_b , the ratio of tilted-surface to horizontal beam radiation, can be found from equation (1.7.1) of [15]. \bar{I}_T , the monthly-average hourly radiation incident on a surface of any orientation, is then given by

$$\bar{I}_T = \bar{R} \bar{I} \quad (\text{B8})$$

